Studies on the Structure−Activity Relationship of Endostatin: Synthesis of Human Endostatin Peptides Exhibiting Potent Antiangiogenic Activities

Francesco Chillemi* and Pierangelo Francescato

Department of Organic and Industrial Chemistry, University of Milan, Via Venezian, 21, 20133 Milano, Italy

Enzio Ragg

Department of Agrifood Molecular Sciences, University of Milan, Via Celoria, 2, 20133 Milano, Italy

Maria Grazia Cattaneo, Sandra Pola, and Lucia Vicentini

Department of Pharmacology, School of Medicine, University of Milan, Via Vanvitelli, 32, 20129 Milano, Italy

Received March 26, 2003

The aim of the present research was to study the relationship between chemical structure and antiangiogenic activity of endostatin. Four peptides, containing about 40 amino acid residues, designed to cover nearly the whole sequence of endostatin, were synthesized by the solid-phase method. They were termed Fragment I (sequence 6−49), II (sequence 50−92), III (sequence 93−133), and IV (sequence 134−178), with the latter bearing the original disulfide bond Cys135-Cys165. These peptides were tested for their ability to inhibit endothelial cell proliferation, migration, and both in vitro and in vivo angiogenesis assays in matrigel. Fragments I and IV inhibited cell proliferation and cell migration with a potency and an efficacy higher than that of the full length endostatin. Fragment I was also active in inhibiting in vitro the formation of tubules and in vivo the vascularization of the matrigel. Fragments II and III were devoid of antiangiogenic activity. We propose to use the peptides 6−49 and 134−178 as angiogenesis inhibitors in substitution of full length endostatin, in therapeutic applications for cancer, rheumatoid arthritis, and retinopathies.

Introduction

The remarkable results obtained by the J. Folkman research group[1,2] on angiogenic inhibitors encouraged us to undertake a series of studies on the relationship between chemical structure and the antiangiogenic activity of angiostatin[3] and endostatin.[4] Initially we concentrated our attention on the endostatin rather than angiostatin because of the lower structural complexity of the former. To this end we synthesized four peptide fragments containing about 40 amino acid residues, to cover nearly the whole sequence of human endostatin. Comparison of human, murine, rat,[5] and chicken[6] endostatin sequences and knowledge of the tertiary structure[7,8] was of aid in identifying the topology and size of fragments to be synthesized, so as to include the probable active core(s) in only one fragment.

N. Yamaguchi et al.[9] showed that some endostatin mutants, lacking the N- and/or C-terminal pentapeptide sequences, inhibited angiogenesis with the same potency as the full length endostatin. For this reason, we omitted the N- and C-terminal pentapeptides in our syntheses.

Table 1 shows the sequences of the four synthesized peptides. Fragment I (sequence 6−49) possesses the most conservative sequence among the four above-mentioned species. In addition, this fragment contains a 14-amino acid region (a.a. 26−39), found in the crystal structure of endostatin[7,8] in an α-helical conformation, with the side-chain of two hydrophobic residues (Phe31 and Phe33) unusually located on the protein surface, residues whose side chains are fully exposed to solvent. Fragment II (sequence 50−92) contains a short α-helical segment between Trp83 and Ala87. Fragment III (sequence 93−133) is found in the crystal structure in five β-sheets connected by unstructured segments and constitutes a strongly basic domain with four arginine and three lysine residues. In fragment IV (sequence 134−178) a disulfide bond connects Cys135 and Cys165. This S−S bond limits the molecular flexibility of the fragment and is expected to stabilize the structure, as found in the solid state, formed by two β-sheets connected by a twisted loop.

Results

Peptide Synthesis. Solid-phase peptide synthesis was used in the synthesis of endostain fragments, employing continuous flow technique, Fmoc strategy, and polyethylene-oxide-polystyrene resins. Cys33 in fragment I was protected with Acm, and Cys173 in fragment IV was protected with tBu, to avoid undesirable disulfide bridge formation involving these amino acids. We have purposely terminated fragment 134−178 with Phe178, thus omitting Met179, a residue sensitive to iodine oxidation, necessary for the disulfide bond formation. The yields in the synthesis of this peptide were very poor owing to a particularly difficult sequence, the oxidation step for disulfide bridge formation and a double RP-HPLC purification before and after oxidation.

* To whom correspondence should be addressed. Phone: 00-39-2-5031- 4101. Fax: 00-39.2-5031-4072. E-mail: francesco.chillemi@unimi.it.

10.1021/jm0308287 CCC: $25.00
Published on Web 08/07/2003

Table 1. Sequences of the Synthesized Peptides

Fragment I (sequence 6-49). Phe-Gln-Pro-Val-Leu-His-Leu-Val-Ala-Leu-Asn-Ser-Pro-Leu-Ser-Gly-Gly-Met-Arg-Gly-Ile-Arg-Gly-Ala-Asp-Phe-Gln-Cys(Acm)-Phe-Gln-Gln-Ala-Arg-Ala-Val-Gly-Leu-Ala-Gly-Thr-Phe-Arg-Ala-Phe.

Fragment II (sequence 50-92). Leu.Ser.Ser-Arg-Leu-Gln-Asp-Leu-Tyr-Ser-Ile-Val-Arg-Arg-Ala-Asp-Arg-Ala-Ala-Val-Pro-Ile-Val-Asn-Leu-Lys-Asp-Glu-Leu-LeuPhe-Pro-Ser-Trp-Glu-Ala-Leu-Phe-Ser-Gly-Ser-Glu-Gly.

Fragment III (sequence 93-133). Pro-Leu-Lys-Pro-Gly-Ala-Arg-Ile-Phe-Ser-Phe-Asp-Gly-Lys-Asp-Val-Leu-Arg-His-Pro-Thr-Trp-Pro-Gln-Lys-Ser-Val-Trp-His-Gly-Ser-Asp-Pro-Asn-Gly-Arg-Arg-Leu-Thr-Glu-Ser.

Fragment IV (sequence 134-178). Tyr-Cys-Glu-Thr-Trp-Arg-Thr-Glu-Ala-Pro-Ser-Ala-Thr-Gly-Gln-Ala-Ser-Ser-Leu-Leu-Gly-Gly-Arg-Leu-Leu-Gly-Gln-Ser-Ala-Ala-Ser-Cys-His-His-Ala-Tyr-Ile-Val-Leu-Cys(tBu)-Ile-Glu-Asn-Ser-Phe

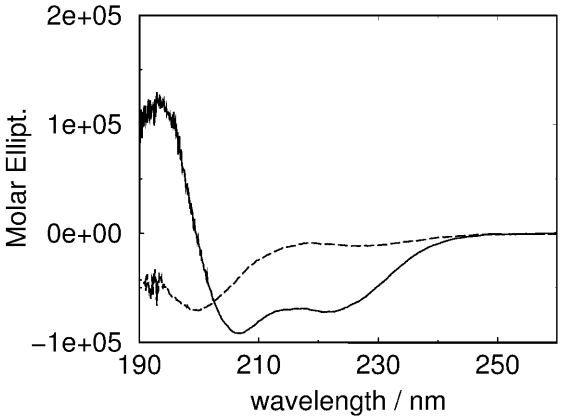

Figure 1. CD spectrum of fragment 6−49, 0.2 mg/mL, 25 °C, in water solution, pH 2.5 (broken line) and in H_2O/TFE 50:50 (v/v) (continuous line).

All peptides synthesized were characterized by RP-HPLC, amino acid analysis, mass spectroscopy, Edman degradation, and some by NMR spectroscopy (see Experimental Section for details).

CD Spectroscopy. CD spectra of fragment 6−49 were recorded in water and water/trifluoroethanol solutions (see Figure 1). Taking into consideration standard values of mean residue molar ellipticities measured at 222 nm (4000 deg cm^2 dmol^{-1} and −38 000 deg cm^2 dmol^{-1} for random coil and α-helix secondary structures) and the corresponding experimental values (−2300 deg cm^2 dmol^{-1} and −17 000 deg cm^2 dmol^{-1}), the α-helical contributions on the secondary structure for fragment I were estimated at 15% and 55%, respectively, for water and water/TFE solutions.

These estimates do not, however, take into account contributions coming from other secondary structures, such as β-turns and β-strands. A more accurate analysis, based of the complete deconvolution of the CD spectra, gave the following results: 7% α-helix, 32% β-strand, 25% β-turn, 36% random coil for water solution; 29% α-helix, 16% β-strand, 21% β-turn, 34% random coil for water/TFE solution at pH 2.5.

No significant change in the molar ellipticity was observed for the water/TFE solution, when the pH was changed from 2.5 to 6.7 by addition of 50 mM phosphate buffer. The crystal structure of human endostatin[7,8] contains a α-helical segment between Ile26 and Ala39. This corresponds to a 30% α-helical contribution in fragment 6−49. Clearly, the peptide dissolved in water has a low amount of α-helix, but its tendency to form α-helical secondary structures is enhanced by the addition of TFE, whose structuring properties are well-known.[10] Segments 10−15 and 45−49 are found in the crystal structure as β-sheet and are connected to the α-helix by large unstructured segments; however, the β-sheet conformation is stabilized by hydrogen-bonding with another segment located in the C-terminus region (a.a 171−176), which in the peptide 6−49 is lacking. It may be possible that these regions still maintain an extended secondary structure in fragment 6−49, given the CD results for the peptide in water as well as in water/TFE solution (20−30% extended secondary structure, corresponding to 9−13 amino acids).

^{1}H NMR Spectroscopy. ^{1}H NMR spectra were performed in water solution at pH 2.5 with or without addition of trifluoroethanol. Many characteristic amino acid spin-systems were immediately recognized from the analysis of 2D-TOCSY and 2D-NOESY experiments. Although a thorough analysis of the secondary structure needs completion of the ^{1}H NMR sequential assignments, the presence and extent of a helical structure was judged by the observed number of HN(i)−HN(i+1) interactions, involving long stretches of residues,[11] observed in the 2D-NOESY spectrum performed in water/TFE 50:50 (v/v) solution and are in qualitative agreement with the CD results. (Figure 2). The addition of TFE was determinant for the acquisition of good quality 2D-NMR spectra and the observation of sequential HN−HN interactions.

In contrast with Fragment I, the ^{1}H NMR spectrum of Fragment IV, dissolved in water, was characterized by extensive line-broadening and a small chemical-shift dispersion of the amide resonances, thus suggesting the

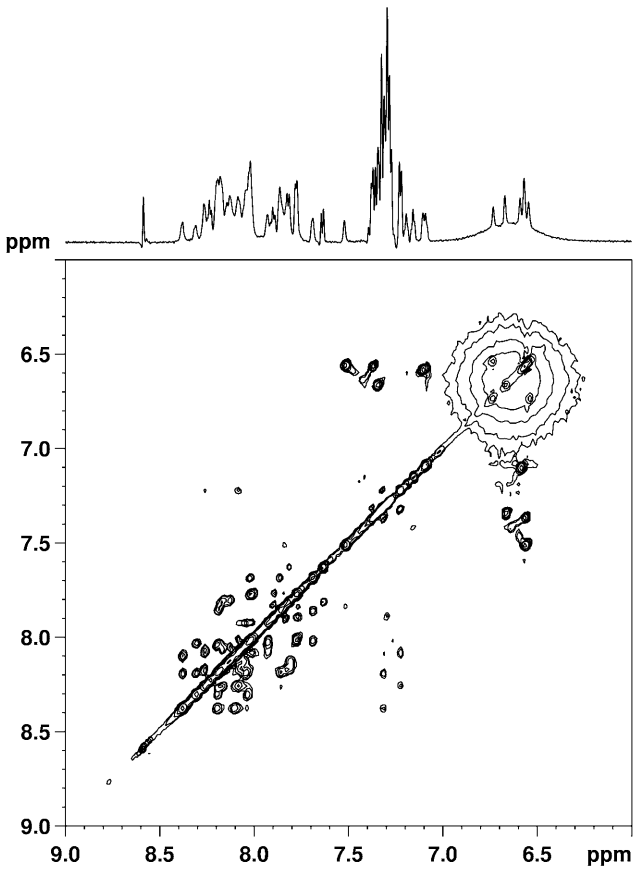

Figure 2. Expansion of a ^{1}H,^{1}H 2D-NOESY spectrum performed at 600 MHz (t_{mix} = 0.24 s, 25 °C) on fragment 6−49, 5 mg/mL H_2O/TFE-d_2 50:50 (v/v), 25 °C, pH 2.5. Amide and aromatic proton region.

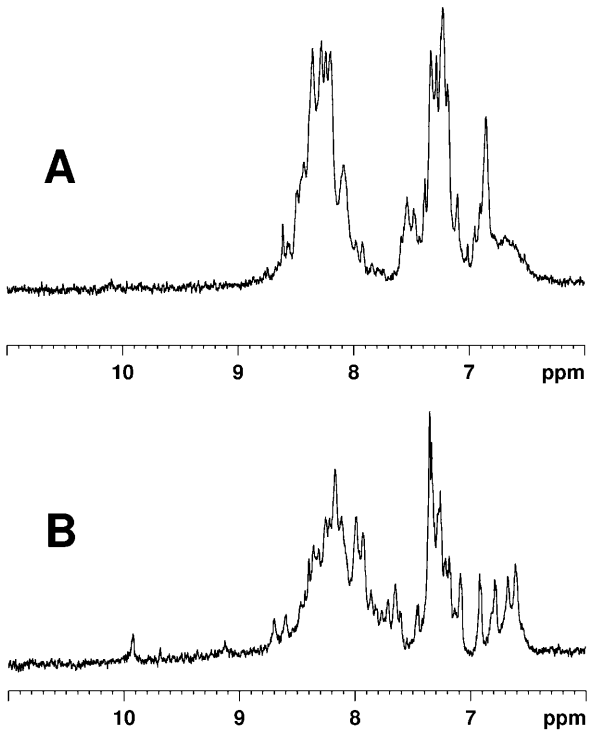

Figure 3. 600 MHz ^{1}H NMR spectrum of fragment 134−178, 5 mg/mL, 25 °C, in H_2O−D_2O 90:10 (v/v) solution (trace A) and in H_2O/TFE 50:50 (v/v) (trace B).

presence of high molecular-weight aggregates (Figure 3 trace A). The addition of trifluoroethanol promotes the partial formation of secondary structure, as judged by some variations in chemical shift for the downfield NH region (Figure 3, trace B). In water/TFE solution the indolic NH resonance of the unique Trp residue at position 138 became evident. It might be that the addition of TFE partially disrupts the aggregates thus decreasing the overall molecular correlation time and the ^{1}H resonance line-widths. The 2D-NOESY spectra, nevertheless, remained featureless.

Cell Proliferation Assay. The inhibition of endothelial cell proliferation induced by the peptides 6−49 and 134−178 was tested by ^{3}H-incorporation. Serum-deprived HUVECs were treated for 48 h with increasing concentrations of the peptides in the presence of 20 ng/mL VEGF as a proangiogenic stimulus. Both peptides inhibited tritiated thymidine incorporation in a dose-dependent manner (Figure 4, parts A and B). Concentrations necessary for half-maximal inhibition (IC_{50}) were 5×10^{-16} M for fragment 6−49, and 5×10^{-15} M for fragment 134−178. The suppression of endothelial cell proliferation by the peptide 6−49 was complete while the peptide 134−178 reached a lower level of inhibition (about 60%). Figure 4C shows the same type of experiment performed using increasing concentrations of full length human endostatin to compare its potency and efficacy with those displayed by the synthetic peptides. Endostatin was less potent ($IC_{50} = 5 \times 10^{-13}$) than both peptides and was of a similar efficacy in comparison with fragment 134−178. The results are the mean values ± SEM of 3−5 independent experiments. Both peptides also inhibit the endothelial cell proliferation stimulated by bFGF (data not shown).

Cell Migration Assay. To assess the cell migration effects of peptides 6−49, 134−178, and full length endostatin, a Boyden chamber and the VEGF as chemoattractant was used. The angiogenic factor induced human umbilical vein endothelial cell (HUVEC) migration with increases of 2.12 ± 0.4 (n = 8) fold above basal values (in the absence of chemiotactic agent, 19.9 ± 5 cell/field, n = 8). The addition of increasing concentrations of peptides and endostatin to the cell suspension in the Boyden's upper chamber induced a dose-dependent inhibition of cell migration with an IC_{50} of 3×10^{-13} M for the 6−49 fragment, of 8×10^{-13} M for fragment 134−178, and of 5×10^{-12} M for endostatin (Figure 5, parts A, B, and C). The maximal inhibition of the chemotactic response was 60% for 6−49 and 40% for 134−178 and endostatin. None of the tested peptides or endostatin concentrations altered cell migration in the absence of the chemoattractants.

Fragments 50−92 and 93−133 in the assays described above were devoid of antiangiogenic activity.

Since the peptide 6−49 seems to be some more potent and more efficaciuos than fragment 134−178 and owing to the small quantity of this at one's disposal, from now on the following in vitro and in vivo experiments were performed using fragment 6−49 only.

Chemoinvasion Assay. The chemoinvasion experiments were performed as described under Experimental Section and requires the digestion of a layer of matrigel by the invading cells. HUVECs stimulated with VEGF (50 ng/mL) were able to penetrate through a matrigel barrier during the 6 h of the assay (35.9 ± 2.86 cells/

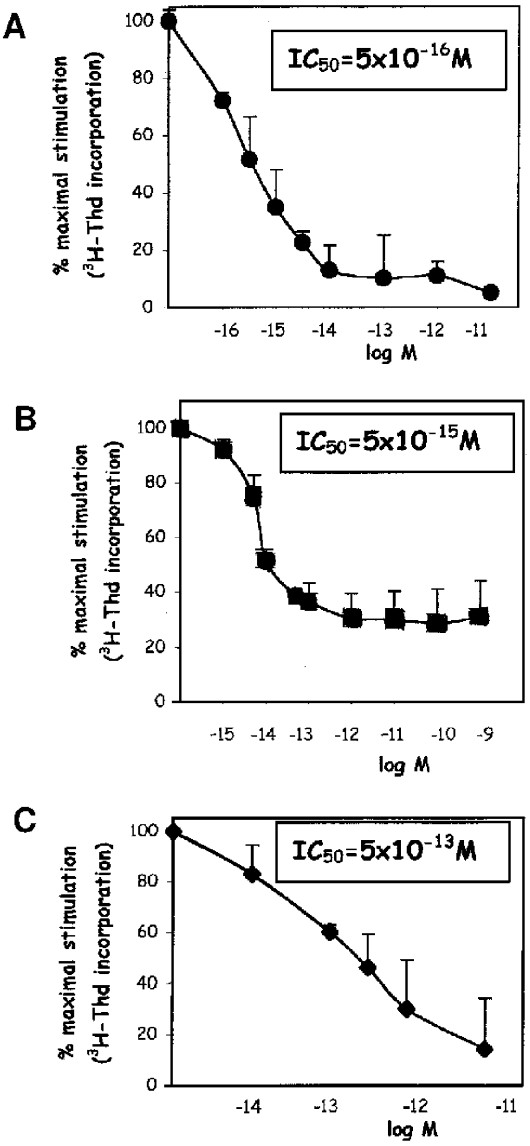

Figure 4. Inhibition of endothelial cell proliferation by fragments 6−49 (A) and 134−178 (B) in comparison with endostatin (C).

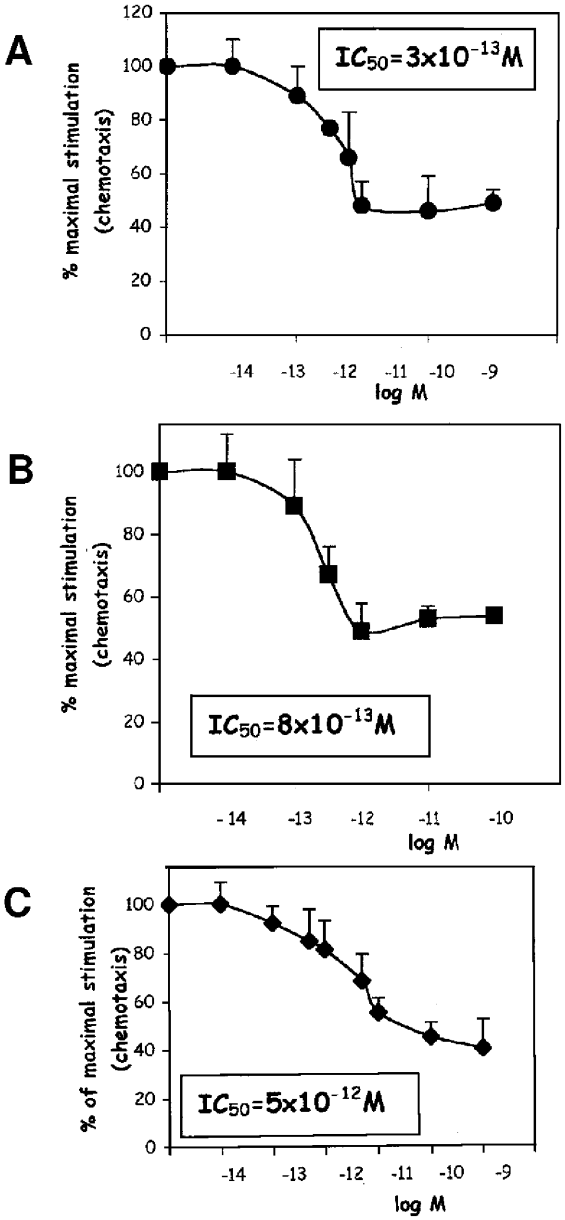

Figure 5. Inhibition of endothelial cell migration by fragments 6−49 (A) and 134−178 (B) in comparison with endostatin (C).

field; basal levels = 12.9 cells/ field ± 1.65; n = 4). Application of a maximal dose of the peptide 6−49 (10 nM) reduced the invasion process by 48 ± 4%. Endostatin at the same concentration induced an inhibition of 53 ± 3% (data not shown).

In Vitro Angiogenic Assay. In vitro endothelial cells plated on matrigel enriched with angiogenic factors form a three-dimensional network of tubes resembling capillary-like structures. HUVECs preincubated with 1 nM of the peptide 6−46 for 30 min were then plated on a layer of polymerized matrigel in the presence of FGF and VEGF as described in the Experimental Section. Peptide 6−49 was present during the entire length of the assay (12−18 h). The treatment resulted in an inhibition of endothelial cell alignment and cord formation (Figure 6B) in comparison with the control (Figure 6A). Quantification by optical imaging of the area occupied by the capillary network showed that maximal tube formation observed in the control cells, and considered 100%, was reduced to 23% in the presence of peptide 6−49.

In Vivo Angiogenic Assay. The antiangiogenic in vivo activity of peptide 6−49 and endostatin was assessed using the matrigel plug assay. The seven week old female mice were subcutaneously injected with 0.5 mL of matrigel enriched with 75 ng/mL of aFGF and 30 units of heparin. Peptide 6−49 or endostatin were mixed with FGF and heparin in the matrigel at a final concentration of 20 nM. Within 4 days the formation of hemorragic lesion in the matrigel pellets was evident in the control. Treatment with both compounds visibly reduced the neovascularization process (Figure 7). Quantification of vascularization by determination of hemoglobin content of matrigel sponges showed that peptide 6−49 significantly inhibited (P < 0.01) FGF-induced angiogenesis when added to matrigel (4.96 ± 0.11 g/dL in the control vs 1.75 ± 2.01 in animals treated with peptide and 3.42 ± 2.51 with endostatin). This experiment demonstrated that peptide 6−49 is more potent than the endostatin on either a weight or a molar

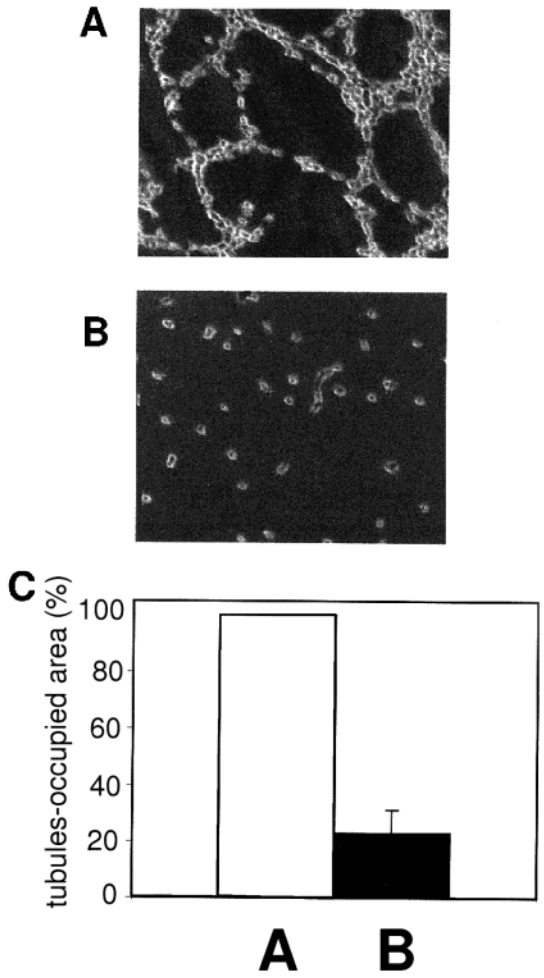

Figure 6. In vitro angiogenesis: inhibition of the capacity of endothelial cells to form tubular structures (B) when treated with peptide 6-49 in comparison with the control cells (A) and quantification of the results (C) by NIE image.

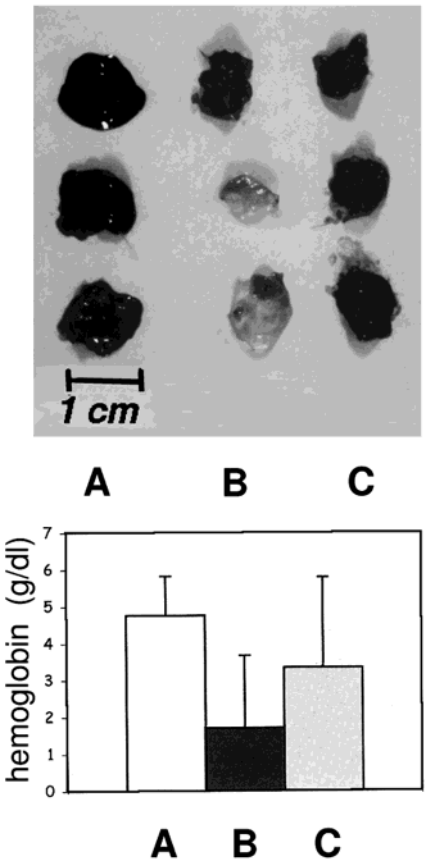

Figure 7. In vivo angiogenesis: hemoglobin levels in matrigel pellets (top) and quantificatin of hemoglobin (g/dL) content in pellets (bottom). (A) Control animals. (B) Animals treated with peptide 6−49 at 20 nM. (C) Animals treated with endostatin at 20 nM.

basis (approximately 8 and 2 times, respectively). A previous paper of only biological results was published by Cattaneo M. G. et al.[12]

Discussion

In the present research we have shown that two synthetic fragments, corresponding to sequence 6−49 and 134−178 of human endostatin, exhibit potent antiangiogenic activities. These peptides inhibited cell proliferation and cell migration with a potency and an efficacy even higher than native endostatin. Our results show effects of these peptides at very low concentrations. Fragment 6−49 inhibited in vitro the capacity of endothelial cells to form tubular structures similar to capillaries and was also capable of reducing hemoglobin levels in matrigel pellets, which indicates a decreased formation of vessels in animals treated with peptide compared with controls and with endostatin. On the contrary, the peptides corresponding to sequences 50−92 and 93−133 were devoid of antiangiogenic activity.

The cellular mechanisms by which endostatin induces its effects are not yet elucidated. Fragments 6−49 and 134−178 behave differently in solution, as shown in the NMR spectra, and therefore seem to possess a different secondary structure. This suggests that conformational and structural properties of individual peptides are able to modulate their biological activity and that the two peptides probably produce their antiangiogenic effects through distinct mechanisms. It has recently been found that endostatin, when subjected to denaturation/renaturation steps, is a protein with a high propensity to form amyloid aggregates, characterized by Congo Red-staining and birifrengence, and that these aggregates are cytotoxic to murine neuroblastoma cells in vitro.[13] Indeed, our NMR experiments provide a first indication for a greater propensity of fragment IV to aggregate; thus, this endostatin segment might be involved in the onset of amyloid formation.

It is also surprising that two peptides are more active than endostatin. Similar examples are not lacking in the literature. Let it suffice to cite the instance of cholecystokinin in which the C-terminal octapeptide is several times more potent than the native hormone with 33 amino acid residues, on either molar or weight basis.[14]

In the case of endostatin, a recent report[15] has shown that fragment 90−134 of murine endostatin possesses in vivo a potent angiogenic effect, inducing neovascularisation of the rabbit cornea. Its activity in promoting angiogenesis was comparable in intensity and in its temporal profile to that of VEGF. Peptide 90−134 enhances, in an additive fashion, the angiogenic response to the VEGF when the two compounds were coreleased in the same cornea, providing firm evidence of its proangiogenic activity.

In light of this result, the reasons may be explained for which the peptides 6−49 and 134−178 have an antiangiogenic activity higher than full length endostatin and at least partly for which the first clinical trials of endostatin yielded results inferior to expectation.[16,17]

In conclusion, the use of endostatin synthetic fragments, besides allowing study of the relationship between chemical structure and antiangiogenic activity, could simplify the studies of its cellular mechanisms of action. In addition, fragments 6−49 and 134−178, alone or in mixture, may be exploited for therapeutic applications proposed for angiogenesis inhibitors (cancer, rheumatoid arthritis, and retinopathies), as substitutes for the full length endostatin, which also contains a proangiogenic domain in its interior; this partly antagonizes the effects of antiangiogenic domains. Last, the addition of peptide 6−49 to the conventional chemotherapic carmustine enhances antitumoral efficacy in rat gliomas (model 9L), exercising a remarkable synergism.[18]

The results of present research were patented on behalf of Milan University.[19] Another previous patent[20] reports the antiangiogenic activities of murine endostatin fragments.

Experimental section

Abbreviations. Fmoc, 9-fluorenylmethoxycarbonyl; Boc, *tert*-butyloxycarbonyl; Pbf, 2,2,4,6,7-pentamethyldihydrobenzofuran-5-sulfonyl; Trt, trityl; tBu, *tert*-butyl; HOBt, 1-hydroxybenzotriazole; PyBop, (benzotriazol-1-yloxy)tripyrrolidinophosphonium hexafluorophosphate; Acm, acetamidomethyl; DIPEA, *N*-diisopropylethylamine; 2D-NOESY, two-dimensional-nuclear overhauser enhancement spectroscopy; 2D-TOCSY, two-dimensional-total correlation spectroscopy; FBS, fetal bovine serum: BSA, bovine serum albumin; VEGF, vascular endothelial growth factor; FGF, fibroblast growth factor.

Materials. Fmoc-amino acids and Fmoc-amino acid-pentafluorophenyl esters were purchased from Sigma-Aldrich, Milan, Italy, and from Chem-Impex International Inc., Wood Dale, IL. Fmoc-amino acid-NovaSyn TGA resins, dye Novachrome, PyBop, and endostatin were obtained from Calbiochem-Novabiochem AG, Laufefingen, Switzerland. Collagen type I and matrigel were purchased from Becton Dickinson, Bedford, MA. VEGF 165 and FGF were obtained from PeproTech Inc., Rocky Hill, NJ, and Sigma Chemicals, St. Louis, MO, respectively. [^{3}H]Thymidine (specific activity 2 Ci/mmol) came from Amersham Pharmacia Biotech, UK. Tissue culture reagents were purchased from Sigma Chemical, St Louis, MO.

Peptide Synthesis. Solid-phase synthesis was carried out on an automated peptide synthesizer (Biolynx plus, mod 4170, Novabiochem, Nottingham, UK). The functional groups of lateral chains of amino acids were protected as follows: Arg-(Pbf), Asp(OtBu), Cys33 by Acm, Cys135 and Cys165 by Trt, Cys173 by tBu, Glu(OtBu), His(Trt), Lys(Boc), Ser(tBu), Thr-((tBu), Trp(Boc) and Tyr(tBu).

Fmoc-amino acid-NovaSyn TGA resin (0.01 mmol) was suspended in 30 mL of DMF and after 2 h was loaded in the reaction column. The Fmoc-amino acid resins were then subject to the following treatments: (a) washings with DMF; (b) removal of Fmoc by using a 20% piperidine solution in DMF; (c) washings with DMF; (d) coupling in DMF with suitable Fmoc-amino acid-pentafluorophenyl ester (5 equiv) in the presence of HOBt (5 equiv) as catalyst, with addition of anionic dye Novachrome for automatically monitoring the reaction time. Only in the case of Fmoc-Arg(Pbf) and Fmoc-His(Trt), the carboxyl was activated by using PyBop (1 equiv), HOBt (1 equiv) and DIPEA (2 equiv), without addition of dye (reaction time 4 h). All coupling reactions were repeated; (e) washings with DMF. After completion of the chain assembly, the synthetic peptide-resin was washed sequentially with DMF, *tert*-amyl alcohol, acetic acid, *tert*-amyl alcohol, dichloromethane, and diethyl ether; the peptide resin was then dried under vacuum.

Table 2. Yields, Physicochemical, and Analytical Data for Endostatin Fragments I−IV

	fragment			
	I	II	III	IV
yield	20%	17%	21%	3%
$[\alpha]^{20}_D$[a]	−74.5°	−71.2°	−77.0°	−44.1°
MS (calcd)[b]	4777.5	4820.7	4671.2	4854.2
MS (found)	4777.0	4821.0	4671.0	4854.0
Asp[c]	2.10(2)	3.91(4)	3.88(4)	1.03(1)[c]
Thr	0.98(1)	-	2.03(2)	2.92(3)
Ser	1.99(2)	5.82(6)	3.95(4)	-
Glu	4.11(4)	4.05(4)	2.03(2)	5.91(6)
Pro	1.82(2)		4.87(5)	0.95(1)
Gly	6.12(6)	2.07(2)	4.12(4)	3.89(4)
Ala	5.96(6)	3.95(4)	0.99(1)	5.93(6)
Cys	0.96(1)	-	-	2.82(3)
Val	2.98(3)	3.03(3)	2.10(2)	0.93(1)
Met	0.95(1)		-	-
Ile	1.10(1)	1.96(2)	1.02(1)	2.17(2)
Leu	4.93(5)	6.88(7)	3.07(3)	4.91(5)
Tyr	-	0.98(1)	-	-
Phe	4.89(5)	2.07(2)	1.96(2)	1.05(1)
His	0.87(1)	-	-	1.87(2)
Arg	3.96(4)	3.87(4)	3.89(4)	1.95(2)
Trp	-	1.11(1)	2.13(2)	0.87(1)
Lys	-	-	3.06(3)	-

[a] Optical activity ($c = 0.1$, H_2O). [b]Molecular mass. [c]Amino acid analysis (expected values in brackets). Purity of each peptide was >95% based on RP-HPLC. The homogeneity of synthesized peptides was also estimated by complete Edman degradation using a sequenator; the results show only expected amino acid residues.

Deprotection and cleavage of peptides from resin were performed with a mixture of TFA 87%, thioanisole 5.5%, ethanedithiol 2.5%, phenol 2.5%, and water 2.5%. The mixture was left to react for 2 h at room temperature with occasional stirring. After filtration under vacuum, the resin was washed twice with TFA. The filtrate was cooled in ice and added slowly under stirring with dry diethyl ether to precipitate the polypeptide. The product was filtered, repeatedly washed with dry diethyl ether, and finally dried under vacuum over KOH.

For removal of the two *S*-trityl groups with concomitant disulfide bond formation between Cys135 and Cys165, fragment IV (140 mg) was dissolved in 200 mL of 75% methanol, and then a solution of 12 mg of iodine in 80 mL of 75% methanol was added dropwise while stirring. The reaction solution was added with a 10% solution of ascorbic acid until complete decolorization of iodine. Methanol was thoroughly evaporated off under vacuum, and the remaining aqueous solution was lyophilized.

The crude polypeptides were purified by semipreparative reverse-phase HPLC using a Aktabasic 100 instrument (Amersharm Pharmacia Biotech, Friburg) and a Jupiter column (250 × 21.2 mm) 15 μm, C 18, 300 Å (Phenomenex, Torrance, CA). The polypeptides were dissolved in solvent A (0.1% aqueous TFA + 10% acetonitrile) and eluted with a gradient of solvent B (90% acetonitrile + 10% of 0.1% aqueous TFA). The flow rate was 20 mL/min, and the detection was set at 226 nm. Main fractions were pooled and lyophilized.

The purified polypeptides were characterized by amino acid analysis, analytical RP-HPLC (Jupiter column, 250 × 10 mm, 10 μm, 300 Å), and mass spectrometry using a Thermo Finnigan instrument mod LCQ Deca XP. For Edman degradation, the sequenator " Procise" mod 491 from Applied Biosystems (Foster City, CA) was employed. Yields and physicochemical and analytical data of the synthesized peptides are reported in Table 2.

Circular Dichroism Spectroscopy. CD spectra were recorded on a Jasco J-810 (Jasco International Co. Ltd. Tokio, Japan) spectropolarimeter equipped with a thermoelectrically controlled cell holder. CD data were deconvoluted

using the CDNN software v. 2.1 (downloaded from http://bioinformatik.biochemtech.unihalle.de/cdnn). The peptide concentration was 0.26 mM.

NMR Spectroscopy. NMR samples were prepared by dissolving 5 mg of peptide in 0.6 mL of H_2O/D_2O 90:10 (v/v) or H_2O/trifluoroethanol-d_2 50:50 (v/v). No buffer or salt was added. The pH was 2.5 for water solutions. Deuterated solvents were purchased from Isotec, Miamisburg, OH with 99.9% isotopic purity. Solutions were transferred immediately into a 5-mm NMR tube (Wilmad 535-PP). All experiments were performed on a Bruker AMX-600 spectrometer (Bruker Spectrospin AG, Rheinstetten, Germany) equipped with a 5-mm reverse-detection probe. Chemical shifts were measured in δ (ppm) using as external reference sodium 2,2-dimethyl-2-silapentane-5-sulfonate.

2D-NOESY and 2D-TOCSY experiments were performed in phase-sensitive mode using standard pulse programs. Spin-lock was achieved with an MLEV-17-based pulse-sequence with duration between 40 ms and 60 ms. Solvent suppression was achieved by presaturation, using a long (duration 1.3s) low-power RF pulse set on resonance during the relaxation delay and, in the case of NOESY spectra, during the mixing-time. Typical acquisition parameters were 1024 × 4K free induction decays acquired using 9090 Hz spectral width, 48 scans. Spectra were transformed in phase-sensitive mode, with a 90° shifted sine-bell squared weighting function and zero-filling to 2K × 2K real data points. A 5th order polynomial was applied in both dimensions for baseline correction.

Cell Culture. Human umbilical vein endothelial cells (HUVECs) isolated from umbilical cords as previously described,[21] were maintained in culture in 199 medium, supplemented with 20% heat-inactivated FBS, 25 μg/mL endothelial cell growth factor, and 50 μg/mL heparin.

Cell Proliferation Assays. HUVECs in serum-deprived 199 medium were inoculated in 96 well-plates at a density of 2×10^4 cells/well and pretreated for 30 min with endostatin or its fragments. The cells were then stimulated for 48 h with 20 ng/mL VEGF, and tritiated thymidine (1 μCi/well) was added during the last 6 h of incubation. The cells were then extracted in 10% TCA, and the radioactivity incorporated in the TCA insoluble fraction was determined after solubilization in 0.5 M NaOH.

Migration and Chemoinvasion Assays. Cell migration was assessed in a 48-well microchemotaxis chamber using Nuclepore polyvinylpyrrolidine (PVP)-free polycarbonate filters of 8 μm porosity. The filters were coated with 50 μg/mL of human fibronectin and were placed over a bottom chamber containing VEGF as chemoattractant factor. Serum-free medium containing 0.1% fatty acid-free BSA was employed as negative control. HUVECs, suspended in DMEM medium containing 0.1% fatty acid free BSA, were pretreated for 30 min with endostatin or its fragments and then added to the upper chamber at a density of 5×10^4 cells/well in the presence of the drug. The chamber was incubated at 37 °C for 6 h. At the end of incubation, nonmigrated cells on the upper surface of the filter were removed by a scraper. The cells migrated to the lower side of the filter were colored with Diff-quick stain (VWR Scientific Products, Bridgeport, NJ). Migrated cells were then counted in six different fields per filter at 160× magnification with a microscope (Zeiss). The assays were run in triplicate.

For the chemoinvasion assay, the filters were coated with a layer of matrigel (100 μg/filter), and the Boyden chamber was assembled with the coated side of the filter facing the cells in the upper compartment. The assays were then performed as described for chemotaxis.

In Vitro Angiogenesis Assays. Capillary-like structures formation was evaluated by plating endothelial cells at a density of 5×10^4 cells/well on a layer of polymerized matrigel. VEGF (10 ng/mL) and basic FGF (10 ng/mL) were used as angiogenic stimuli. Peptide 6−49 was added to the cells 30 min before detachment and was present in the medium during the incubation. The plates were incubated at 37 °C in 5% CO_2, for 18 h, and the cells were then fixed in 4% paraformaldehyde. The images were acquired using an Axiovert microscope (Zeiss) with a PCO SuperVGA SensiCam (Axon Instruments Inc., Union City, CA). The degree of cord formation was quantified by measuring the area occupied by the tubes in five random fields from each well using the National Istitute of Health (NIH) Image Program.

In Vivo Angiogenesis Assays. Matrigel sponge model of angiogenesis introduced by Passaniti et al.[22] and Albini et al.[23] was used. Matrigel (500 μL) containing 150 ng of acid FGF and 60 units/mL of heparin were slowly injected subcutaneously in the abdominal region of female mice C57/b16, of age from 6 to 8 weeks (Charles River, Calco, LC, Italy). Fragment 6−49 or endostatin were added to the matrigel at a final concentration of 20 nM. In vivo, the gel quickly polymerized to form a solid gel. After 4 days, mice were sacrificed, the matrigel pellets were recovered, and the amount of hemoglobin therein was measured by means of a commercial kit based on Drabkin's method (Sigma, St. Louis, MO).

Acknowledgment. This work was supported by grants from Ministero dell'Università e della Ricerca Scientifica e Tecnologica (MURST 40% and 60%), Roma, Italy. We would like to thank Prof. Paolo Mantegazza, Magnificus Rector of Milan University, for financial contributions. We are indebted with Dr. Stefania Iametti for the execution of CD spectra and with Dr. Ivano De Noni for mass spectra.

Supporting Information Available: HPLC profiles and mass spectra for fragments I and IV. TOCSY spectum for fragment I. This material is available free of charge via the Internet at http://pubs.acs.org.

References

(1) O'Reilly, M. S.; Boehm, T.; Shing, Y.; Fukai, N.; Vasions, G.; Lane, W. S.; Flynn, E.; Birkhead, J. R.; Olsen, B. R.; Folkman J. Endostatin: an endogenous inhibitor of angiogenesis and tumor growth. *Cell* **1997**, *88*, 277−285.

(2) Kisker, O.; Becker, C. M.; Prox, D.; Fannon, M.; D'Amato, R.; Flynn, E.; Fogler, W. E.; Lee Sim, B. K.; Allred, E. N.; Pirie-Shepherd, S. R.; Folkman J. Continuous administration of endostatin by intraperitoneally implanted osmotic pump improves the efficacy and potencyof therapy in a mouse xenograft tumor model. *Cancer Res.* **2001**, *61*, 7669−7674.

(3) Cao, Y.; Ji, R. W.; Davidson, D.; Schaller, J.; Marti, D.; Sohndel, S.; McCance, S. G.; O'Reilly, M. S.; Llinàs M.; Folkman, J. Kringle domains of Angiostatin. *J. Biol. Chem.* **1996**, *271*, 29461−29467.

(4) Oh, S. P.; Warman, M. L.; Seldin, M. F.; Cheng, S. D.; Knoll, J. H. M.; Timmons, S.; Olsen B. R. Cloning of cDNA and genomic DNA encoding human type XVIII collagen and localization of the α1(XVIII) collagen gene to mouse chromosome 10 and human chromosome 21. *Genomics* **1994**, *19*, 494−499.

(5) Perletti, G.; Concari, P.; Giardini, R.; Marras, E.; Piccinini, F.; Folkman, J.; Chen, L. Antitumor activity of endostatin against carcinogen-induced rat primary mammary tumor. *Cancer Res.* **2000**, *60*, 1793−1796.

(6) Dong, S.; Cole, G. J.; Halfter, W. Expression of collagen XVIII and localization of its glycosaminoglycan attachment sites. *J. Biol. Chem.* **2003**, *278*, 1700−2003.

(7) Hohenester, E.; Sasaki, T.; Olsen, B. R.; Timpl, R. Crystal structure of the angiogenesis inhibitor endostatin at 1.5 Å resolution. *EMBO J.* **1998**, *17*, 1656−1664.

(8) Ding, Y. H.; Javaherian, K.; Lo, K. M.; Chopra, R.; Boehm, T.; Lanciotti, J.; Harris, B. A.; Li, Y.; Shapiro, R.; Hohenester, E.; Timpl, R.; Folkman, J.; Wiley: D. C. Zinc-dependent dimers observed in crystals of human endostatin. *Proc. Natl. Acad. Sci. U.S.A.* **1998**, *95*, 10443−10448.

(9) Yamaguchi, N.; Anand-Apte, B.; Lee, M.; Sasaki, T.; Fukai, N.; Shapiro, R.; Que, I.; Lowik, C.; Timpl, R.; Olsen, B. R. Endostatin inhibits VEGF-induced endothelial cell migration and tumor growth independently of zinc binding. *EMBO J.* **1999**, *18*, 4414−4423.

(10) Luo, P.; Baldwin, R. L. Mechanism of helix induction by trifluoroethanol: a framework for extrapolating the helix-forming properties of peptides from trifluoroethanol/water mixtures back to water. *Biochemistry* **1997**, *36*, 8413−8421.

(11) Wüthrich, K. *NMR of Proteins and Nucleic Acids*; John Wiley & Sons: New York, 1986; pp 162−166.

(12) Cattaneo, M. G.; Pola, S.; Francescato, P.; Chillemi, F.; Vicentini, L. M. Human endostatin-derived synthetic peptides possess potent antiangiogenic properties in vitro and in vivo. *Exp. Cell Res.* **2003**, *283*, 230−236.
(13) Kranenburg, O.; Kroon-Batenburg, M. G.; Reijerkerk, A.; Wu. Y.; Voest, E. E.; Gebbink, M. F. B. G. Recombinant endostatin forms amyloid fibrils that bind and are cytotoxic to murine neuroblastoma cells in vitro. *FEBS Lett.* **2003**, *539*, 149−155.
(14) Rubin, B.; Engel, S. L.; Drungis, A. M.; Dzelzkalns, M.; Grigas, E. O.; Waugh, M. H.; Yiacas, E. Cholecystokinin-like activities in guinea pigs and in dogs of C-terminal octapeptide (SQ 19.844) of cholecystokinin. *J. Pharm. Sci.* **1969**, *58*, 955−959.
(15) Morbidelli, L.; Donnini, S.; Chillemi, F.; Giachetti, A.; Ziche, M. Angiosuppressive and angiostimulatory effects exerted by synthetic parzial sequences of endostatin. *Clin. Cancer Res.* **2003** (in press).
(16) Herbst, R. S.; Hess, K. R.; Tran, H. T.; Tseng, J. E.; Mullani, N. A.; Charnsangavej, C.; Madden, T.; Davis, D. W.; McConkey, D. J.; O'Reilly, M. S.; Ellis, L. M.; Pl, R.; Pluda, J.; Hong, W. K.; Abbruzzese, J. L. Phase I study of recombinant human endostatin in patient with advanced solid tumors. *J. Clin. Oncol.* **2002**, *20*, 3792−3803.
(17) Eder, J. P.; Supko, J. G.; Clark, J. W.; Puchalski, T. A.; Garcia-Carbonero, R.; Ryan, D. P.; Shulman, L. N.; Proper, J.; Kirvan, M.; Rattner, B.; Connors, S.; Keogan, M. T.; Janicek, M. J.; Fogler, W. E.; Schnipper, L.; Kinchla, N.; Sidor, C.; Phillips, E.; Folkman, J.; Kufe, D. W. Phase I clinical trial of recombinant human endostatin administered as a short intravenous infusion repeated daily. *J. Clin. Oncol.* **2002**, *20*, 3772−3784.
(18) Pradilla, G.; Legnani F. G.; Tyler, D. M.; Chillemi, F.; Francescato, P.; Brem, H.; Olivi, A.; DiMeco, F. Enhanced antitumour efficacy by combining carmustin with endostatin peptide 6−49 in an intracranial glioma model. Manuscript in preparation.
(19) Chillemi, F.; Vicentini, L.; Francescato, P. PCT Patent. International Publication Number: WO 02/068457 A2. Applicant: University of Milan. Antiangiogenic peptides. Priority Data: 27.02.2001 (esp@cenet).
(20) Chillemi, F.; Francescato, P.; Ziche, M. PCT Patent. International Publication Number: WO 00/63249. Applicants: University of Milan and University of Florence. Polypeptides derived from endostatin exhibiting antiangiogenic activity. Priority Data: 15.04.1999 (esp@cenet).
(21) Jaffe, E. A.; Nachman, R. L.; Becker, C. G.; Minck, C. R. Culture of human endothelial cells derived from umbilical veins. Identification by morphologic and immunologic criteria. *J. Clin. Invest.* **1973**, *52*, 2745−2756.
(22) Passaniti, A.; Taylor, R. M.; Pili, R.; Guo, Y.; Long, P. V.; Haney, J. A.; Pauly, R. R.; Grant, D. S.; Martin, G. R. A Simple, quantitative method for assessing angiogenic and antiangiogenic agents using reconstituted membrane, heparin and fibroblast growth factor. *J. Neurosurg.* **1992**, *77*, 519−528.
(23) Albini, A.; Fontanini, G.; Masiello, L.; Tacchetti, C.; Bigini, D.; Luzzi, P.; Noomam, D. M.; Sterler-Stevenson, W. Angiogenic potential in vivo by Kaposi sarcoma cell-free supernatants and HIV1-tat product: inhibition of KS-like lesions by TIMP-2. *AIDS (London)* **1994**, *8*, 1237−1244.

JM0308287